Direct observations of dislocations in thermotropic smectics using freeze-fracture replication

Joseph A. N. Zasadzinski

J. Phys. France **51** (1990) 747-756 15 AVRIL **1990**, PAGE 747

Classification
Physics Abstracts
61.30E — 61.30J — 61.16D

Direct observations of dislocations in thermotropic smectics using freeze-fracture replication

Joseph A. N. Zasadzinski

Department of Chemical and Nuclear Engineering, University of California, Santa Barbara CA 93106, U.S.A.

(*Reçu le 18 septembre 1989, accepté sous forme définitive le 12 décembre 1989*)

Résumé. — Les méthodes modernes de trempe suivie de réplication par fracture sont idéales pour la visualisation directe de la structure tridimensionnelle et des défauts dans les phases cristal liquide smectique et cholestérique. La résolution y est proche des distances moléculaires. On a trempé le nonanoate de cholestérol à partir du voisinage de la transition smectique-cholestérique pour mettre en évidence des couches smectiques étendues et bien définies, distordues par des dislocations coins et vis ayant une densité très élevée. Les dislocations vis ont des vecteurs de Burgers de couche unique organisée comme des parois twistées. Il est tentant de penser que le twist présent dans la phase cholestérique induit un twist résiduel dans la phase smectique qui est incompatible avec la mise en forme de couches. On a observé aussi des boucles de dislocations vis-coin organisées également en parois twistées. On a suggéré que ces parois soient responsables de la disparition de l'ordre smectique amenant la phase cholestérique.

Abstract. — Modern rapid-freezing methods followed by freeze-fracture replication techniques are ideally suited to allow the direct visualization of the three-dimensional structure and defects of thermotropic smectic and cholesteric liquid crystalline phases with resolution approaching molecular dimensions. Cholesterol nonanoate was quench frozen from near the smectic-cholesteric transition to reveal extensive, well defined smectic layers distorted by a high density of screw and edge dislocations. The screw dislocations typically had Burgers vectors of a single layer and commonly organized as twist walls. This is suggestive that the twist present in the cholesteric phase induces a residual twist in the smectic phase incompatible with perfect layering. Screw-edge dislocation loops were also commonly observed, also organized into twist walls. These twist walls have been suggested as being responsible for the breakdown of smectic ordering leading to the cholesteric phase.

Introduction.

Smectic and cholesteric phases and the phase transition from smectic to cholesteric (or nematic) has been extensively studied by a variety of experimental techniques, most notably by optical microscopy and X-ray and light scattering techniques [1, 2]. Unfortunately, none of these techniques reveal the structure, number, or interactions of defects such as dislocations that might be important to the stability of these phases, or may even mediate the phase

transitions. Freeze-fracture electron microscopy, however, is ideally suited for investigations of the defect structure in liquid crystals [3], and has been used extensively in investigations of lyotropic nematic, smectic and lamellar phases [3-12]. Freeze-fracture electron microscopy can be usefully applied to thermotropic liquid crystals, although there are far fewer examples in the literature [13-16]. This may be due to the more complex fracture behavior of thermotropic materials as compared to the multiphase dispersions normally investigated with freeze-fracture techniques [16]. However we show here that for smectic phases, the fracture appears to follow the layers as is observed in lyotropic smectics and the fracture patterns relate simply to the molecular order in these phases. The defect structure is visible to near molecular dimensions and edge and screw dislocations are easily seen. The freeze-fracture technique may be an important tool for studies of unusual smectic phases including the recently hypothesized smectic-A* phase [17, 18].

Materials and methods.

The most important step in any freeze-fracture investigation of high vapor pressure materials is the initial rapid freezing or quench step [3]. Cholesterol nonanoate (CN) (recrystallized from solvent) was provided by J. Goodby. A small droplet (0.1-0.5 μl) of CN heated to the isotropic phase was sandwiched between two copper planchettes (Balzers BUO-12-056T ; Hudson, NH) to form a 10-50 μm thick layer. Previously, the copper planchettes had been etched for 1 s in concentrated nitric acid to remove any contamination and roughen the planchette surfaces. The apparatus used for freezing was a modified version of a Balzers Cryojet QFD 020 jet freeze device [21]. The sample sandwiches were mounted on a Teflon support arm and placed in a temperature controlled oven located vertically over the jets of the freezing device. Sample temperature was controlled prior to freezing to better than 0.1 °C. The samples were equilibrated at the appropriate temperature for a few minutes before a solenoid-actuated mechanism opened a Teflon door at the bottom of the oven and dropped the Teflon arm and samples between the opposed jets of the Balzers cryojet. A photodiode switch initiated the high velocity flow of liquid propane, cooled by liquid nitrogen to – 180 °C, which impinged on the copper sandwich from both sides to provide a minimum average cooling rate of 15 000 °C/s. The initial cooling rate, which is most important for preserving phases of limited temperature range, is likely to be somewhat slower for the first few degrees of cooling [22]. The frozen copper sandwiches were stored under liquid nitrogen until transferred into a spring-loaded « mousetrap » carrier. The loaded sample carrier was mounted onto the liquid nitrogen-cooled coldfinger in a Balzers 400 freeze-etch device and the vacuum chamber was evacuated to better than 10^{-7} torr. The temperature of the sample carrier and coldfinger were adjusted to – 170 °C and the spring mechanism was externally actuated, thereby fracturing the samples. The fracture surfaces were immediately replicated by evaporating 1.5 nm of a platinum carbon mixture from an electrode at a 45° angle to the fracture surface, followed by a 15 nm thick film of carbon at normal incidence to increase the mechanical stability of the replica. The samples and replicas were removed from the vacuum chamber and the samples and copper planchettes were dissolved in chromic acid, leaving the platinum-carbon replicas behind [23]. The replicas were washed in chloroethanol-water mixtures, rinsed in doubly-distilled water, and collected on formvar-coated 50 mesh gold electron microscope grids (Pelco, Tustin, California). The replicas were examined in a JEOL 100 CX scanning transmission electron microscope in the conventional transmission mode using 80 kV electrons. Images were recorded on Kodak electron image plates. Shadows (absence of platinum) appear light in the prints.

Results and discussion.

Cholesterol nonanoate forms a cholesteric phase at 91 °C and a smectic-A phase at 73 °C on cooling [19]. The untwisting of the helical pitch of the cholesteric phase near the smectic-A transition is well known [19]. The cholesteric twist is incompatible with the layered textures of the smectic-A phase ; hence the twist and bend elastic constants diverge along with the cholesteric pitch at the transition [19, 20]. The smectic phase does not supercool or appear to grow by nucleation of smectic domains as the transition is second order. Hence, the transition is difficult to capture using rapid freezing followed by freeze-fracture techniques and we could not observe the untwisting of the helical pitch. However, we were able to freeze in the cholesteric phase from 77 °C (Fig. 1). Samples frozen from 75 °C showed intermediate textures (Fig. 2) and were difficult to interpret. Samples frozen from approximately 1 °C below the transition temperature (Figs. 3-5) showed well defined smectic layering punctuated by numerous screw and edge dislocation defects.

To interpret freeze-fracture images of thermotropic liquid crystals it is necessary to relate the fracture surface to the molecular structure. Berreman *et al.* [16] proposed that in a spatially varying, anisotropic, brittle material, the specific surface energy was directly related to the number of molecules separated by the advancing crack. This is equivalent to saying that the binding energy per molecule is independent of the molecular orientation. Each molecule is assumed to occupy an ellipsoidal volume that reflects the local anisotropy of the fluid. In nematic or cholesteric liquid crystals, the molecules spontaneously align along a preferred direction. The ratio of the major to minor axes of the ellipsoid is related to the molecular alignment of the material. A crack normal to the major axis of the ellipsoid separates more molecules that a crack parallel to it ; hence the fracture would prefer to propagate along the major axis of the ellipsoids, providing that the new area created was not too large. The

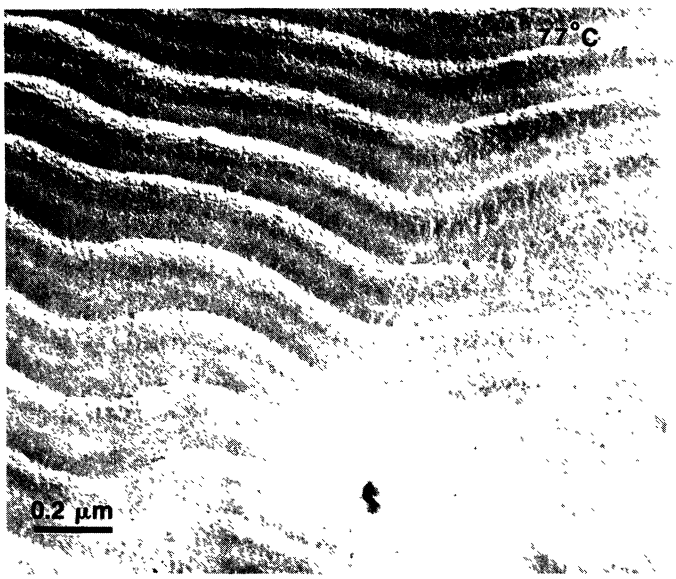

Fig. 1. — Freeze-fracture image of cholesterol nonanoate (CN) quenched from 77 °C. The fracture surface is typical of the cholesteric phase. The regular undulations of spacing 130-140 nm is a measure of the half pitch of the cholesteric twist. See reference [16] for explanation of fracture pattern.

product of surface area and this specific surface energy was calculated by Berreman for cholesteric and blue phase liquid crystals using anisotropy parameters measured independently by optical diffraction or predicted by theory (cf. Berreman *et al.* [16]) and the computed fracture patterns matched those observed in cholesteric and blue phases quite closely. For smectic phases, however, the layering imposes a density modulation that appears to influence the crack propagation more than the local orientation. The fracture surface propagates primarily between layers, the region of lowest density, as is observed for lyotropic smectics [3, 4].

Figure 1 is a freeze-fracture electron microscope image of CN frozen from 77°. The images showed textures typical of other cholesteric phases we have imaged previously [13, 15, 16]. The regular undulating fracture surface is related to the regular twisting of the molecules along the cholesteric axis. These undulations can extend for several microns before the cholesteric axis or the fracture surface changes directions. Calculations by Berreman *et al.* [16] suggest that this pattern is the result of fracture roughly normal to the cholesteric axis, and that the undulation period of about 130-140 nm is roughly equivalent to half of the cholesteric pitch. This is in good agreement with the results of Pindak *et al.* [19] who measured an optical pitch of 360 nm (the optical pitch is related to the actual pitch by $P_{\text{optical}} = nP_{\text{actual}}$, in which n is the average refractive index, here about 1.5-1.6). It was somewhat surprising that we were able to visualize the cholesteric phase as the transition to the smectic phase is continuous and does not supercool. Apparently, the finite time necessary for diffusion and rearrangement in these viscous materials is sufficient to allow us to lock in high temperature phases even if the lower temperature phase does not form by a first order transition, provided that the cooling rate is rapid enough.

Samples frozen from 75 °C revealed a mixture of smectic-like and cholesteric-like fracture patterns. Figure 2 shows one such region in CN in which the undulations characteristic of the

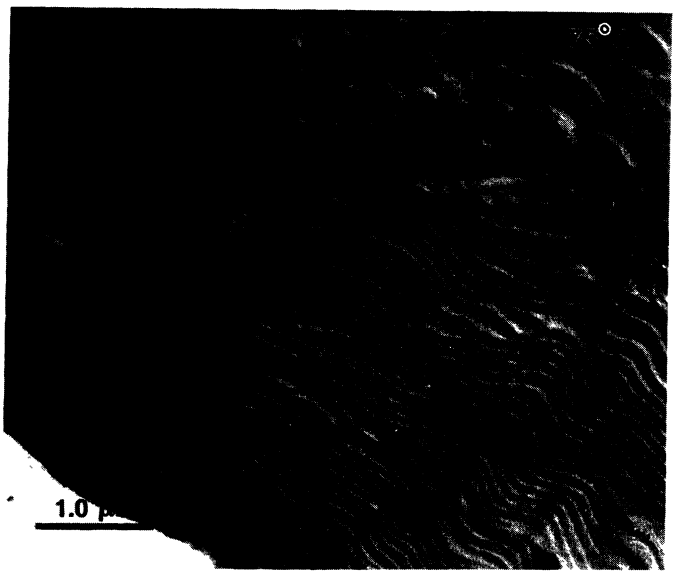

Fig. 2. — Freeze-fracture image of CN quenched from 75 °C. The fracture surface is much less regular than figure 1 and appears to be a mixture of smectic and cholesteric textures. The irregular spacing of the undulations may be related to fluctuations associated with the phase transition, or with temperature gradients present in the sample during quenching.

cholesteric phase at the bottom of the image give way to a smoother, almost layer-like structure at the top of the image. The undulations in the cholesteric are not as uniform as they are in the samples frozen from higher temperatures (see Fig. 1). There are often gaps between undulations and the cholesteric pitch is not well defined. It is not clear if this region represents the textures that result from fluctuations during the unwinding of the cholesteric pitch as it transforms to the smectic phase, of if there was a small temperature gradient across the sample during freezing resulting in a mixture of smectic and cholesteric textures. The cholesteric pitch more than doubles when CN is cooled slowly from 75° to 74° [19], and eventually diverges as the temperature is lowered to 73 °C. Previously, we have shown (22) that a rough estimate of the maximum temperature gradient across the sample thickness is

$$(T_s - T_c)\frac{Bi}{2}$$

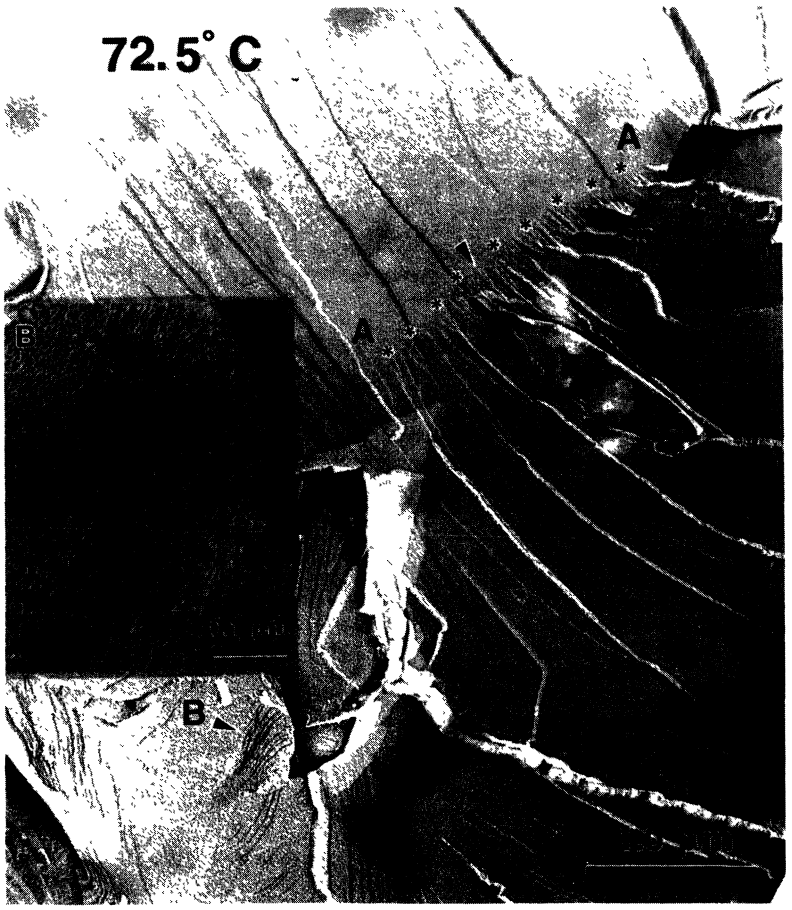

Fig. 3. — Freeze-fracture image of CN quenched from 72.5 °C. The fracture surface is that of well-defined layers punctuated by numerous dislocation defects. A twist wall of screw dislocations is located along the asterisks between A's. A small arrow marks where one of these screw dislocations pierces the fracture surface. Screw-edge dislocation loops are present at B. In the magnified inset of B, the twist wall abruptly changes the layer organization from being roughly parallel to the fracture plane to almost perpendicular to the fracture plane.

in which Bi is the Biot modulus of the sample (hd/k, h is the heat transfer coefficient, d is the sample half-thickness, and k is the sample thermal conductivity), and $T_s - T_c$ is the difference between sample and cryogen temperatures. For a typical sample, Bi = 0.01-0.02, hence the maximum gradient across the sample thickness is about 1-2 °C. Laterally, we expect the gradients to be of the same magnitude as the entire surface of the sample is contacted simultaneously by a stream of liquid propane cooled by liquid nitrogen. This uniform exposure to the cryogen, coupled with the high conductivity of the copper support should minimize any lateral temperature gradients. In the samples frozen from 77 °C, we saw no variation in the pitch of the cholesteric helix across the samples, which is consistent with this approximation.

Figures 3-5 are typical of samples frozen from 72.5 °C. Figure 3 shows a low magnification view of flat layers punctuated by numerous edge and screw dislocation networks. Between defects, the layers appear flat, which is not completely expected as the smectic-A phase is known to be better described by a density modulation than by well defined layers [1, 2]. This may be the result of the limited vertical resolution of the freeze-fracture image or by some enhancement of layer ordering due to the freezing process. The low temperatures may quench any fluctuations in the layer thickness, resulting in better defined layers. Smooth variations in vertical topography < 1 nm in height are difficult to resolve by metal shadowing, hence small,

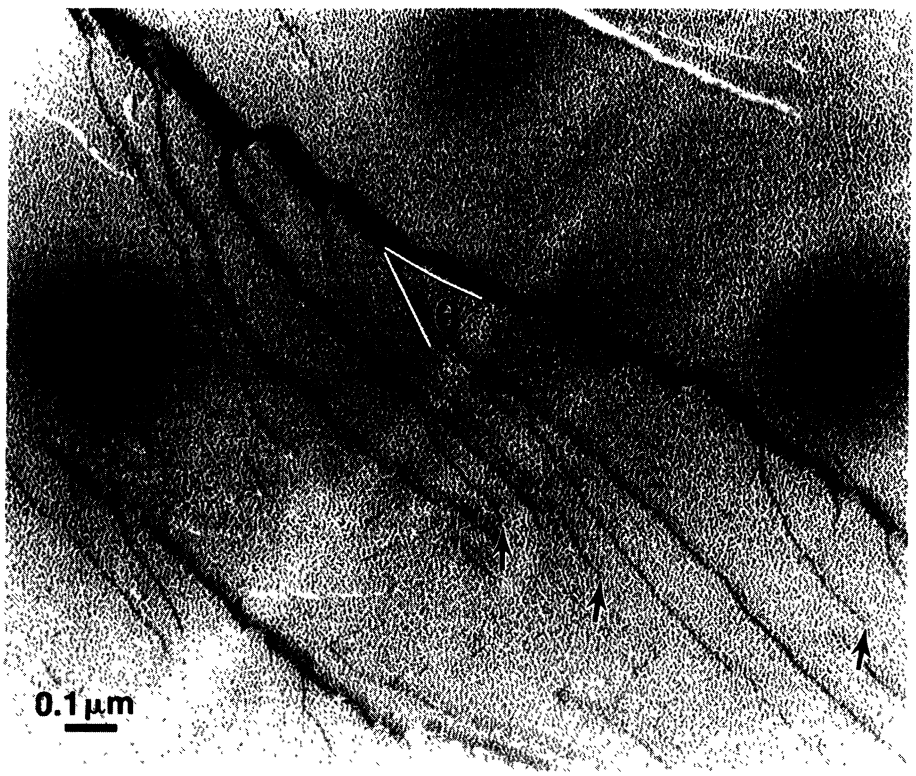

Fig. 4. — Screw dislocation steps in CN frozen from 72.5 °C converging with neighboring steps to form « rivers », with a well-defined coalescence angle, θ. As the rivers coalesce, the apparent thickness of the main « river » grows by the thickness of the tributary « river » added. The arrows show where the individual screw dislocation lines pierce the fracture surface.

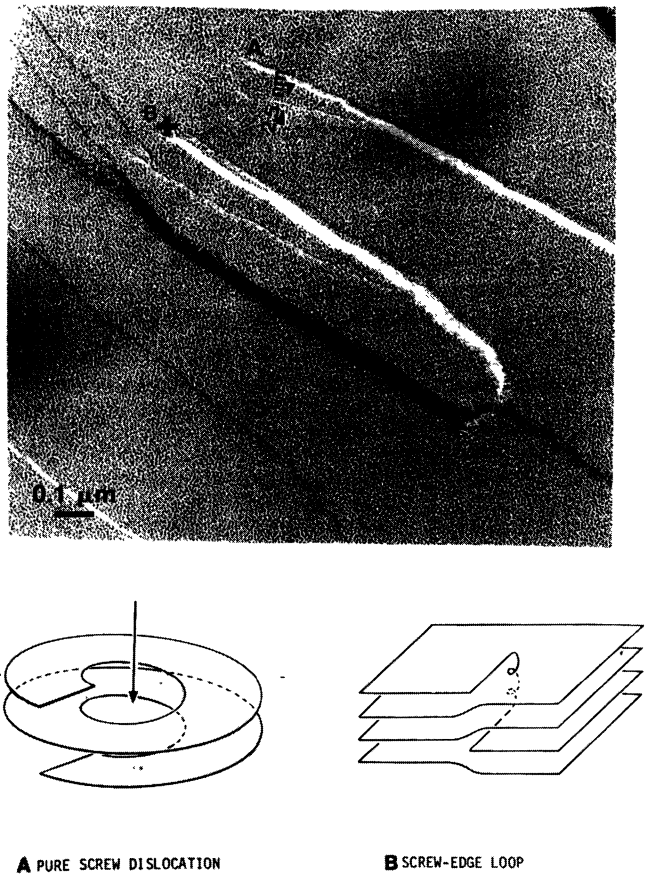

Fig. 5. — A combined screw-edge loop in CN frozen from 72.5 °C. This arrangement is shown schematically in cross section in figure 5b. The screw-edge loop in figure 5 begins at B+ where the screw dislocation line emerges from the fracture plane. The small plateau of additional layers can be thought of as an edge dislocation line with Burgers vector of several layers. The loop ends at B−, where a second screw dislocation line of opposite sign to B+ disappears into the fracture surface. Figure 5a shows schematically a pure screw dislocation line such as the one at A in the freeze-fracture image. Most of the screw dislocations we observed had Burgers vectors of a single layer, about 2.5 nm in thickness.

long wavelength variations in the layer thickness would not be visible in the freeze-fracture images [3]. However, in comparison to similar magnification images of lyotropic smectic phases prepared in identical ways [3, 4], the replicas of CN in the smectic phase appear grainy and perhaps rough on the length scale of the platinum crystallites that make up the replica film (see Figs. 4, 5). This same roughness does not appear in the images of the cholesteric phase (Fig. 1), and might be interpreted as a fine scale variations in the layer thickness. Abrupt steps between single layers, such as the screw dislocations present at the arrows in figures 3-5, are easily visible. The smallest step height (measured by the thickness of the white shadow between the arrows in Fig. 5) is approximately 2.5 nm, or roughly one molecular length.

As has been predicted for smectic-A phases [2], and observed for single-phase lyotropic smectics [4, 5], a high density of screw dislocations are found. A screw dislocation in a smectic phase resembles a spiral staircase, with the dislocation line being the axis of the staircase (see Fig. 5a and Fig. 5.20 of Ref. [2]). The dislocation can be thought of as being formed by cutting a stack of layers perpendicular to the layers, then reattaching each cut edge to the layer above (or below) it. In a freeze fracture image, a screw dislocation appears as either a light or dark line which terminates abruptly into an unbroken layer at the point where the screw dislocation line pierces the fracture surface (arrows in Figs. 3, 4). The dark and light lines are caused by the shadowing effect of the metal deposition on the step produced where the dislocation pierces the fracture surface. Because of the choice of shadow angle relative to the sample plane, the length of the shadow at these steps is roughly equal to the height of the step (this assumes that the local fracture plane is roughly parallel to the sample plane). Hence, the Burgers vector of the dislocation is roughly equivalent to the thickness of the shadow on the images. Most of the screw dislocations appear to have Burgers vectors of one or at most a few layers, and the sign of the Burgers vector can be assigned by the shadow pattern at the step, dark and light shadows corresponding to dislocations of opposite signs. Screw dislocations of small Burgers vector, **b**, are predicted as their energy goes as [2] :

$$E_s = \frac{B\mathbf{b}^4}{128\,\pi^3 r_c^2}$$

in which B is the elastic compressibility modulus and r_c is a core radius.

As the screw dislocation steps propagate along the fracture surface, they often converge with neighboring steps to form « rivers », with a well-defined coalescence angle as shown in figure 4 ([24], also Figs. 5.19 and 5.20 in Ref. [2]). As the rivers coalesce, the apparent thickness of the main « river » grows by the thickness of the tributary « river » added. This increase (or decrease for dislocations of opposite sign) in the river thickness corresponds to an equivalent increase in the step height, because of the metal shadowing. The increases in step height between the layers result in a tilt between the layers on opposite sides of the step. The average tilt between the layers is given by $\delta = \mathbf{b}/d$, in which **b** in the Burgers vector of the screw dislocation (about 25 Å), and d is the average distance between unit screw dislocations. These twist boundaries between layers might be a way of incorporating the residual twist of the cholesteric phase, while still maintaining the layered structure of the smectic phase [2, 17, 18]. In CN at 72.5 °C, we often found large numbers of screw dislocations of similar sign aligned in long rows (Fig. 3, asterisks). Screw dislocations aligned in this way can form twist walls, allowing the layering direction to change direction over relatively short distances. Such twist walls are visible along the asterisks between A's in figure 3. These twist walls may be result of the proximity of the cholesteric phase ; the twist wall is one way of making a degree of twisting compatible with the layered structure of the smectic phase. Kléman suggests that twist walls may be associated with the transition from smectic to cholesteric (or nematic) phases. Renn and Lubensky [17] have postulated that regular twist walls of screw dislocations may be responsible for the structure of the newly discovered smectic-A* phase [18], which appears to be a hybrid phase structurally between a normal smectic-A and a normal cholesteric phase.

The topology of dislocations is such that dislocations cannot end or begin within a given sample of material ; dislocation lines must close on themselves to form loops or end at a free surface or another dislocation [2]. Screw dislocations line in smectics are always perpendicular to the smectic layers ; edge dislocation lines are always parallel to the layers. A combined screw-edge loop can be made by connecting two screw dislocations of opposite signs with an edge dislocation. This arrangement is shown in figure 5 and schematically in cross section in

figure 5b. The screwedge loop in figure 5 begins at B+ where the screw dislocation line emerges from the fracture plane. The small plateau of additional layers can be thought of as an edge dislocation line with Burgers vector of several layers. The loop ends at B−, where a second screw dislocation line of opposite sign to B+ disappears into the fracture surface. Such screw-edge loops have also been observed in lyotropic smectics and have a similar appearance [25]. The Burgers vector of screw-edge loops is complicated by the fact that the energy of screw dislocations as shown above is minimized for defects with Burgers vectors of a single layer, while edge dislocations prefer to have multiple layer Burgers vectors. The energy of an isolated edge dislocation is given by :

$$E = \frac{\kappa |\mathbf{b}|}{\gamma} + \frac{\pi \kappa}{2} \left[\ln \frac{|\mathbf{b}|}{2 d_0} \right] + \tau_c ; \qquad \lambda \equiv \left[\frac{\kappa}{B} \right]^{1/2}$$

b is the Burgers vector of the dislocation and τ_c is a core energy independent of **b**. λ is a length, on the order of the bilayer thickness, over which the compressibility (B) and bend elastic moduli (κ) are comparable [1, 2]. This shows that $E(2\,\mathbf{b}) < 2\,E(\mathbf{b})$; hence a single edge dislocation of large Burgers vector is of lower energy than two (or more) edge dislocations of the same total Burgers vector. This promotes a small number of edge dislocations of large Burgers vector. Hence, the Burgers vector of the loop may be some energetic compromise between these two preferences, or the screw dislocation may be dissociated into many smaller screw dislocations that merge together. Several dark steps arrear to converge near B− in figure 5.

Conclusions.

Freeze-fracture electron microscopy have made it possible to see the three-dimensional structure and organization in a wide range of systems that have previously thwarted analysis. Here we present some of the first images of the three-dimensional organization of defects in thermotropic smectic phases near the cholesteric-smectic transition. Screw dislocations are numerous, with most being organized either in twist walls or in screw-edge dislocation loops. The screw dislocations appear to have Burgers vectors of a single layer, as expected from energy arguments. It also appears to be possible to quench in high temperature phases even if the lower temperature phase is entered by a second order transition, if the quench is initiated far enough from the transition temperature. Freeze-fracture electron microscopy should be an ideal tool to investigate other thermotropic and lyotropic liquid crystalline phases, especially the recently discovered smectic-A* phase which is believed to be stabilized by screw dislocations.

Acknowledgements.

I would like to thank J. Goodby, M. J. Sammon, S. Meiboom, D. W. Berreman, and R. Pindak for generous use of their time and talents, their comments and continuing discussions on the role and possibilities of freeze-fracture. The experimental work described here was done at AT & T Bell Labs. The referees were also helpful in clarifying the interpretation of the images. Financial support was provided by the donors of the Petroleum Research Fund, the Exxon Education Foundation, the DuPont Company, and by a National Science Foundation Presidential Young Investigator Award # CBT 86-57444.

References

[1] DE GENNES P. G., The Physics of Liquid Crystals (Oxford University Press, Oxford) 1974.
[2] KLÉMAN M., Points, Lines and Walls (J. Wiley and Sons, New York) 1983.
[3] ZASADZINSKI J. A. N. and BAILEY S., *J. Elect. Mic. Tech.* **13** (1989) 309 ; ROBARDS A. W. and SLEYTR V. B., Low temperature methods in biological electron microscopy, Practical Methods in Electron Microscopy, Ed. A. M. Glauert (Elsevier Press, Amsterdam.) Vol. 10 (1985) pp. 5-133.
[4] KLÉMAN M., WILLIAMS C. E., COSTELLO M. J. and GULIK-KRZYWICKI T., *Philos. Mag.* **35** (1977) 33.
[5] ALLAIN M., *J. Phys. France* **46** (1985) 225.
[6] MAHAILOVIC M., *C. R. Acad. Sci. Paris* **303** (1986) 1069 ; *C. R. Acad. Sci. Paris* **304** (1987) 875-878.
[7] RÜPPEL D. and SACKMANN E., *J. Phys. France* **44** (1983) 1025.
[8] SAMMON M. J., ZASADZINSKI J. A. N. and KUZMA M. R., *Phys. Rev. Lett.* **57** (1987) 2834.
[9] ZASADZINSKI J. A. N., SCRIVEN L. E. and DAVIS H. T., *Philos. Mag. A* **51** (1985) 287-302.
[10] ZASADZINSKI J. A. N., *Biophys. J.* **49** (1986) 1119.
[11] ZASADZINSKI J. A. N. and MEYER R. B., *Phys. Rev. Lett.* **56** (1986) 636.
[12] ZASADZINSKI J. A. N. and SCHNEIDER M. B., *J. Phys. France* **48** (1987) 2001.
[13] COSTELLO M. J., MEIBOOM S. and SAMMON M. J., *Phys. Rev. A* **29** (1984) 2957.
[14] SIGAUD G., MERCIER M. and GASPAROUX H., *Phys. Rev. A Rap. Comm.* **32** (1985) 1282.
[15] ZASADZINSKI J. A. N., MEIBOOM S., SAMMON M. J. and BERREMAN D. W., *Phys. Rev. Lett.* **57** (1986) 364.
[16] BERREMAN D. W., MEIBOOM S., ZASADZINSKI J. A. N. and SAMMON M., *Phys. Rev. Lett.* **57** (1986) 1737.
[17] RENN S. R. and LUBENSKY T. C., *Phys. Rev. A,* in press.
[18] GOODBY J. W., WAUGH M. A., STEIN S. M., CHIN E., PINDAK R. and PATEL J. S., *Nature* **337** (1989) 449.
[19] PINDAK R. S., HUANG C. C. and HO J. T., *Phys. Rev. Lett.* **32** (1974) 43.
[20] LUBENSKY T. C., *J. Chim. Phys.* **80** (1983) 31.
[21] MÜLLER M., MEISTER N. and MOOR H., *Mikroscopie (Wien)* **36** (1980) 129.
[22] ZASADZINSKI J. A. N., *J. Microsc.* **150** (1988) 137.
[23] FETTER R. D. and COSTELLO M. J., *J. Microsc. (London)* **141** (1986) 277.
[24] FRIEDEL J., Dislocations (Pergamon Press, London) 1964, pp. 321-325.
[25] OSWALD P. and ALLAIN M., *J. Phys. France* **46** (1985) 831.